Title

An Investigation of Elastic Waves with Imaginary and Complex Wave Numbers in Hollow Rods

Authors

McNiven, Hugh

Sackman, Jerome

Shah, Arvind

Publication Date

1965-12-01

Structures and Materials Research
Department of Civil Engineering
Division of Structural Engineering
and Structural Mechanics

Report No. 65-14

AN INVESTIGATION OF ELASTIC WAVES WITH IMAGINARY AND COMPLEX WAVE NUMBERS IN HOLLOW RODS

by

H. D. McNiven
Professor of Civil Engineering
University of California
Berkeley, California

J. L. Sackman
Associate Professor of Civil Engineering
University of California
Berkeley, California

and

A. H. Shah
Assistant Professor of Civil Engineering
The Indian Institute of Technology
Kanpur, India

Structural Engineering Laboratory
University of California
Berkeley, California

December 1965

ABSTRACT

In a previous report [1] an approximate theory was developed which governs the relationship between the frequency and propagation constant for axisymmetric waves in hollow rods, and comparison was made for the lowest three branches contained in the theory with the comparable branches from the exact theory when the propagation constant is real.

In this paper the relationship is found when the propagation constant is pure imaginary and when it is complex. Frequency spectra are formed from the roots of the frequency equation of the approximate theory and these roots form a complex branch and a loop on the imaginary plane connecting the second and third spectral lines on the real plane. The imaginary loop and the complex branch are compared to the comparable branches from the exact, three-dimensional theory.

Some general properties of all of the complex branches which appear in the exact theory are established.

I. INTRODUCTION

In a previous report [1] an approximate theory was developed that gives the relationship between frequency and wave-length for trains of axisymmetric waves travelling in infinitely long, hollow cylindrical rods. The theory takes into account the coupling between the longitudinal, lowest radial and lowest axial shear modes and so is valid for a range of frequencies extending from zero to just below the cutoff frequency of the fourth mode, the lowest neglected in the theory.

Now the quality of an approximate theory must be judged by how well the frequencies predicted by it for a given wave length (or propagation constant) match the corresponding frequencies from the exact three-dimensional theory. In both the exact and approximate equations, the frequency must be real but the propagation constant can be real, imaginary, or complex. In [1], frequency spectra were developed to show the comparison between exact and approximate theories when the propagation constant is real.

In this part of the study, spectral lines are developed from both theories for imaginary and complex propagation constants. The approximate theory which includes the three modes and their three spectral lines on the real plane includes one "loop" on the imaginary plane connecting the second and third branches and one complex branch which extends from the second real branch to the plane $\Omega = 0$. The exact theory contains an infinite number of complex branches all of which originate in either the real or imaginary planes, extend downward in complicated ways and all eventually intersect the plane $\Omega = 0$. As the main purpose of the study is to evaluate the approximate theory when the propagation constant is imaginary or complex, only the lowest imaginary loop and the lowest complex branch of the exact theory are explored numerically. However, study shows that all the complex branches have some interesting general properties. When a complex branch intersects either the real or imaginary plane it does so at a point on a branch in the real or imaginary plane where the slope is zero. In addition the complex branch is perpendicular to the plane it intersects. Finally it is established that when all the complex branches intersect the plane $\Omega = 0$, they are perpendicular to it.

II. The Exact and Approximate Frequency Equations

Both the exact and approximate frequency equations were derived in the previous report.

Both equations have the form

$$F\,(\zeta,\ \Omega;\ a^*,\ \upsilon) = 0$$

where
- ζ = propagation constant
- Ω = normalized frequency
- a^* = ratio of outer to inner radii
- υ = Poisson's ratio .

The normalized frequency Ω and the propagation constant ζ are related to the frequency ω and the wave number along the rod γ according to

$$\Omega = \frac{\omega}{V_2} \cdot \frac{a}{\delta} \quad ; \quad \zeta = \gamma \cdot \frac{a}{\delta}$$

where V_2 is the velocity of shear waves

δ is the lowest root of Eq. (24) in Ref. [1] using $\Omega^1{}_s = 1$

a is the inner radius.

The exact equation is in the form of the determinantal equation

$$|C_{ij}| = 0 \ , \ (i, j = 1 - 4)$$

where the i indicates the row and j the column. The elements of the determinant are

$$
\begin{aligned}
C_{11} &= \delta (2\zeta^2 - \Omega^2) Z_o (\delta\alpha) + 2\alpha\lambda_1 Z_1 (\delta\alpha) \\
C_{12} &= \delta (2\zeta^2 - \Omega^2) W_o (\delta\alpha) + 2\alpha W_1 (\delta\alpha) \\
C_{13} &= 2\zeta [\delta\beta Z_o (\delta\beta) - Z_1 (\delta\beta)] \\
C_{14} &= 2\zeta [\delta\beta\lambda_2 W_o (\delta\beta) - W_1 (\delta\beta)] \\
C_{21} &= 2\zeta\alpha\lambda_1 Z_1 (\delta\alpha) \\
C_{22} &= 2\zeta\alpha W_1 (\delta\alpha) \\
C_{23} &= (2\zeta^2 - \Omega^2) Z_1 (\delta\beta) \\
C_{24} &= (2\zeta - \Omega^2) W_1 (\delta\beta) \\
C_{31} &= \delta a^* (2\zeta^2 - \Omega^2) Z_o (\delta\alpha a^*) + 2\alpha\lambda_1 Z_1 (\delta\alpha a^*) \\
C_{32} &= \delta a^* (2\zeta^2 - \Omega^2) W_o (\delta\alpha a^*) + 2\alpha W_1 (\delta\alpha a^*) \\
C_{33} &= 2\zeta [\delta\beta a^* Z_o (\delta\beta a^*) - Z_1 (\delta\beta a^*)] \\
C_{34} &= 2\zeta [\delta\beta a^* \lambda_2 W_o (\delta\beta a^*) - W_1 (\delta\beta a^*)]
\end{aligned}
\qquad (4)
$$

$$C_{41} = -2\zeta\alpha\lambda_1 Z_1 \quad (\delta\alpha a^*)$$

$$C_{42} = -\,2\zeta\alpha W_1 \;(\delta\alpha a^*)$$

$$C_{43} = (2\zeta^2 - \Omega^2)\;\; Z_1\; (\delta\beta a^*) \qquad (4)$$

$$C_{44} = (2\zeta^2 - \Omega^2)\; W_1\; (\delta\beta a^*).$$

The λ's depend on the phase velocity and are given in Table 1, Ref. [1].

The approximate equation is also in the form of a determinant

$$\begin{vmatrix} a_{11} & a_{12} & a_{13} \\ a_{12} & a_{22} & 0 \\ a_{13} & 0 & a_{33} \end{vmatrix} = 0 \qquad (5)$$

where

$$a_{11} = B\eta_2^2\,\delta^2\zeta^2 + 8(k^2 - 1)\eta_1^2 - B\eta_3^2\delta^2\Omega^2$$

$$a_{22} = 2\delta^2(k^2\zeta^2 - \Omega^2)$$

$$a_{33} = 6\left(k^2\,\frac{A^2}{B^2}\,\delta^2\zeta^2 + \frac{24}{B}\,\eta_2^2 - \frac{A^2}{B^2}\,\eta_4^2\delta^2\Omega^2\right) \qquad (6)$$

$$a_{12} = 4\;(k^2 - 2)\;\eta_1\delta\zeta$$

$$a_{13} = 12\;\eta_2^2\;\delta\zeta$$

and

$$A = a^{*2} - 1$$

$$B = a^{*2} + 1. \qquad (7)$$

The η_i (i = 1 - 4) in Eqs. (6) are adjustment factors used to make the spectral lines from the approximate equations match as well as possible the comparable lines from the exact equation.

These adjustment factors are given for various combinations of a^* and ν in Tables II - IV in [1].

The approximate theory governs the relationship between frequency and wave length for the lowest three modes of motion. In the spectrum this relationship is represented by spectral lines; three on the real plane, one "loop" on the imaginary plane and one complex branch. The imaginary branch and the complex branch are the subjects of special attention in this paper in that we wish to ascertain the quality of the approximate theory when the wave number is imaginary or complex. This quality is judged by how close the imaginary and complex branches from the approximate theory lie to the comparable branches from the exact theory.

III. Numerical Analysis

The imaginary loop and the complex branch from the approximate theory are constructed from the roots of Eq. (5). For a particular rod the a^* and ν are established, and for a given value of Ω Eq. (5) represents a bi-cubic equation in ζ. This equation is solved numerically for ζ^2 using an available program for a cubic equation and the appropriate square roots of the pertinent values of ζ^2 give the imaginary and complex values of ζ. Pairs of (ζ,Ω) are used to trace out the branches.

The imaginary loop from the exact theory is not difficult to establish because when the propagation constant is pure imaginary the value of the determinant in Eq. (3) is real. The loop is formed by first assigning imaginary values to ζ and finding the two values of Ω for each ζ representing the bottom and the top of the loop. We start close to the real plane and move in even increments of ζ away from the real plane until the loop is closed. We begin by choosing a small imaginary value of ζ and Eq. (3) is evaluated for uniformly increasing values of Ω. When there is a change of sign of (3) the interval over which this change has occurred is scanned more finely until the lower value of Ω is determined to better than plotting accuracy. We repeat this procedure for the same value of ζ until the second value of Ω is found. We then increase ζ by an increment and find the two values of Ω for the new ζ. We continue this process until the two values of Ω for a given ζ are close to one another indicating the closure of the loop.

The lowest complex branch of each spectrum is obtained from the exact frequency Eq. (3) by assigning a value to Ω and finding the corresponding complex ζ's using the "method of chords". This method is as applicable to equations involving complex variables as it is to equations containing only real variables. It is an iterative process which begins with two initial values of the unknown variable.

For a given a^* and υ, the procedure is started near the $\Omega = 0$ plane and continues upwards using increments of Ω of .05 until the branch nears the real plane.

We start with $\Omega_1 = .05$ and take as the two first approximations $\zeta_1^{(1)}$ and $\zeta_1^{(2)} = \zeta_1^{(1)} + 0.0005$ where $\zeta_1^{(1)}$ is value of ζ taken from the approximate theory with $\Omega = 0$. Using these two approximate values $\zeta_1^{(3)}$ is found and subsequently we use $\zeta_1^{(3)}$ and $\zeta_1^{(2)}$ to find $\zeta_1^{(4)}$: This process is continued until $| \zeta_1^{(n+1)} - \zeta_1^{(n)} | < 10^{-5}$, at which time the iteration is stopped and $\zeta_1^{(n)} = \zeta_1^{(n+1)}$ is taken to be the root of $F(\zeta,\Omega_1) = 0$.

For the next frequency $\Omega_2 = \Omega_1 + .05$ the first two approximate roots are

$\zeta_2^{(1)}$ and $\zeta_2^{(2)} + 0.005$. Here $\zeta_2^{(1)}$ is assigned the value ζ_1 obtained for the previous frequency. The procedure is continued with Ω increasing in increments until the complex branch is within a distance of .001 from the real ζ plane. At this point the mesh on Ω is made finer so that the intersection point with the real plane may be established with great accuracy.

The method of chords is well suited to finding the complex roots in that it converges on a root rapidly. The complex branch is easily traced from the set of pairs of Ω and ζ.

IV. Comparison of the Spectral Lines

The spectral lines for both imaginary and comples propagation constants are established for three rods; $a^* = 2.0$, $\upsilon = .25$; $a^* = 4.0$, $\upsilon = 0.29$; $a^* = 8.0$, $\upsilon = 0.25$, and the spectral lines are compared in Figs. I - III. For all three rods, the two imaginary loops are difficult to distinguish from one another. Only for the first rod is there a discrepancy and it is slight.

For all three rods the complex branches are close to one another except near the frequency Ω^* at which the branch from the exact theory intersects the real plane. For this frequency the surface representing $F(\zeta,\Omega)$ is almost plane, so that the slightest inaccuracy represented by the approximate theory is magnified in this region. The lack of close matching in this one region is a consequence of having to force the matching for the approximate theory at a point on the real plane instead of being able to match the curvatures at the lowest intercept.

V. Properties of the Complex Branches

When the propagation constant is complex, Eq. (1) is complex and may be written

$$F(\zeta, \Omega) = F_1(\xi, \eta, \Omega) + i F_2(\xi, \eta, \Omega). \tag{8}$$

where $\zeta = \xi + i\eta$.

Because for any point on the real plane ($\eta = 0$), $F(\zeta, \Omega)$ is real, we conclude that

$$F_2(\xi, 0, \Omega) = 0. \tag{9}$$

We now consider Eq. (1) for points in a region close to the real plane, i.e., $F(\xi + i\Delta\eta, \Omega)$. We express this function as a Taylor series expansion about the real plane, and if we consider points on the complex branch then

$$F(\xi + i\Delta\eta, \Omega) = 0. \tag{10}$$

If we set the real and imaginary parts of the expansion each equal to zero, use Eq. (9), and retain only the leading terms of each expansion, we find

$$\text{I.} \quad F_1(\xi, 0, \Omega) = 0$$

$$\text{II.} \quad \Delta\eta \frac{\partial F_2}{\partial \eta}(\xi, 0, \Omega) = 0. \tag{11}$$

As $F(\zeta,\Omega)$ is an analytic function, the real and imaginary parts of it must satisfy the Cauchy-Riemann condition

$$\frac{\partial F_2}{\partial \eta} = \frac{\partial F_1}{\partial \xi}$$

and as $\Delta\eta \neq 0$, Eqs. (11) can be written

$$\begin{aligned} &\text{I.} \quad F(\xi, \Omega) = 0 \\ &\text{II.} \quad \frac{\partial F}{\partial \xi}(\xi, \Omega) = 0 \, . \end{aligned} \tag{13}$$

These same properties were found for the Pochhammer equation governing solid rods by Onoe, McNiven, and Mindlin [2].

If we call one set of roots of the first of (13) ξ^* and Ω^* we have from the first of (13) and (10)

$$\begin{aligned} &F(\xi^*, \Omega^*) = 0 \\ &F(\xi^* + i\Delta\eta, \Omega^*) = 0 \quad . \end{aligned} \tag{14}$$

We observe from Eqs. (14) that as we move a small distance from the point (ξ^*, Ω^*) perpendicular to the real plane we remain on a complex branch. We conclude that near the real plane each complex branch is contained in a plane perpendicular to the real plane.

If we expand

$$F(\xi^* + i\Delta\eta, \Omega^* + \Delta\Omega)$$

in a Taylor series about (ξ^*, Ω^*) and use the same steps as before, we find

$$\frac{\partial\Omega}{\partial(i\eta)} = \lim_{\Delta\eta \to 0} \frac{\Delta\Omega}{(i\Delta\eta)} = - \frac{\frac{\partial F}{\partial \xi}(\xi^*, \Omega^*)}{\frac{\partial F}{\partial \Omega}(\xi^*, \Omega^*)} \quad . \tag{15}$$

Now $\frac{\partial F}{\partial \Omega}$ (ξ^*, Ω^*) is not usually zero, but the numerator is zero from the second of Eqs. (13), so

$$\frac{\partial \Omega}{\partial (i\eta)} \quad (\xi^*, \Omega^*) = 0. \tag{16}$$

Thus, the projections of the complex branches on the imaginary plane are perpendicular to the real plane, so that together with the finding above we conclude that the complex branches are perpendicular to the real plane where they intersect it.

The same reasoning as above may be used with

$$\frac{\partial F}{\partial \Omega} \quad \frac{\partial \Omega}{\partial \xi} + \frac{\partial F}{\partial \xi} = 0 \tag{17}$$

to show that

$$\frac{\partial \Omega}{\partial \xi} \quad (\xi, \Omega^*) = 0 \quad . \tag{18}$$

Therefore, the complex branches intersect the real plane at points on the real branches where their slope is zero.

Using the same reasoning as up to this point it can be shown that when the complex branches intersect the imaginary plane, they intersect it normally and at points of the imaginary branches where the slope is zero.

Finally, we find that, except for a single case, the branches are all perpendicular to the plane $\Omega = 0$.

This can be shown by observing that

$$F\ (\zeta, \Omega) = G\ (\zeta^2, \Omega^2) = 0\ . \tag{19}$$

All branches therefore have a mirror image about the plane $\Omega = 0$. Assuming that $G(2, \Omega^2)$ is continuously differentiable with respect to Ω even at $\Omega = 0$, $\zeta \neq 0$, we conclude that the branches must be perpendicular to the plane $\Omega = 0$.

The single exception to this is the lowest branch on the real plane, the "fundamental" branch. We found in [1] that this branch intersects the plane $\Omega = 0$ with a slope equal to $2(1 + \nu)$. Insight into this case is gained by expanding the function

$$G\left[\, g(\bar{\zeta} + \Delta\zeta),\ f(\bar{\Omega} + \Delta\Omega)\right] \tag{20}$$

in a Taylor series about the point $(\bar{\zeta}, \bar{\Omega})$, a root of Eq. (1). Using the steps as outlined above we find that when we equate Eq. (20) to zero we obtain

$$\frac{d\Omega}{d\zeta}(\bar{\zeta}, \bar{\Omega}) = Z(\bar{\zeta}, \bar{\Omega}) \cdot \frac{\bar{\zeta}}{\bar{\Omega}} \tag{21}$$

$$\text{where } Z = \frac{\partial G}{\partial g} \bigg/ \frac{\partial G}{\partial f}\,. \tag{22}$$

Now $Z(\bar{\zeta}, 0)$ is not usually zero or infinity so when $\bar{\Omega} \to 0$, both the real and imaginary parts of the slope $\frac{\partial\Omega}{\partial\zeta}(\bar{\zeta}, 0)$ approach infinity, and thus the branch is perpendicular to the plane $\Omega = 0$. However for the lowest real branch $\bar{\zeta}$ is also zero, so that the slope $\frac{\partial\Omega}{\partial\zeta}(0,0)$ need not be infinite, and indeed is not.

The points at which the complex branches intersect the plane $\Omega = 0$ are not found readily from Eq. (1) in that it is satisfied identically when Ω is zero. The equation giving these points is obtained by expanding Eq. (19) in a Taylor series about the $\Omega = 0$ plane and taking the limit as Ω^2 approaches zero. The resulting equation is

$$\lim_{\Omega^2 \to 0} \frac{\partial G}{\partial \Omega^2} (\zeta^2, \Omega^2) = 0 \ . \tag{23}$$

References

1. H. D. McNiven, A. H. Shah and J. L. Sackman, "An Approximate Theory for the Vibrations of Hollow, Elastic Rods", Report No. 65-13, Structural Engineering Laboratory, University of California, Berkeley, Nov., 1965.

2. Morio Onoe, H. D. McNiven and R. D. Mindlin, "Dispersion of Axially Symmetric Waves in Elastic Rods", JAM. 29 Trans ASME, Series E, Vol. 84, 1962, pp. 729-734.

Captions for Figures

Figures 1-3: Spectra of frequency vs. propagation constant showing comparison between the exact and approximate theories for the imaginary loop and the complex branch.

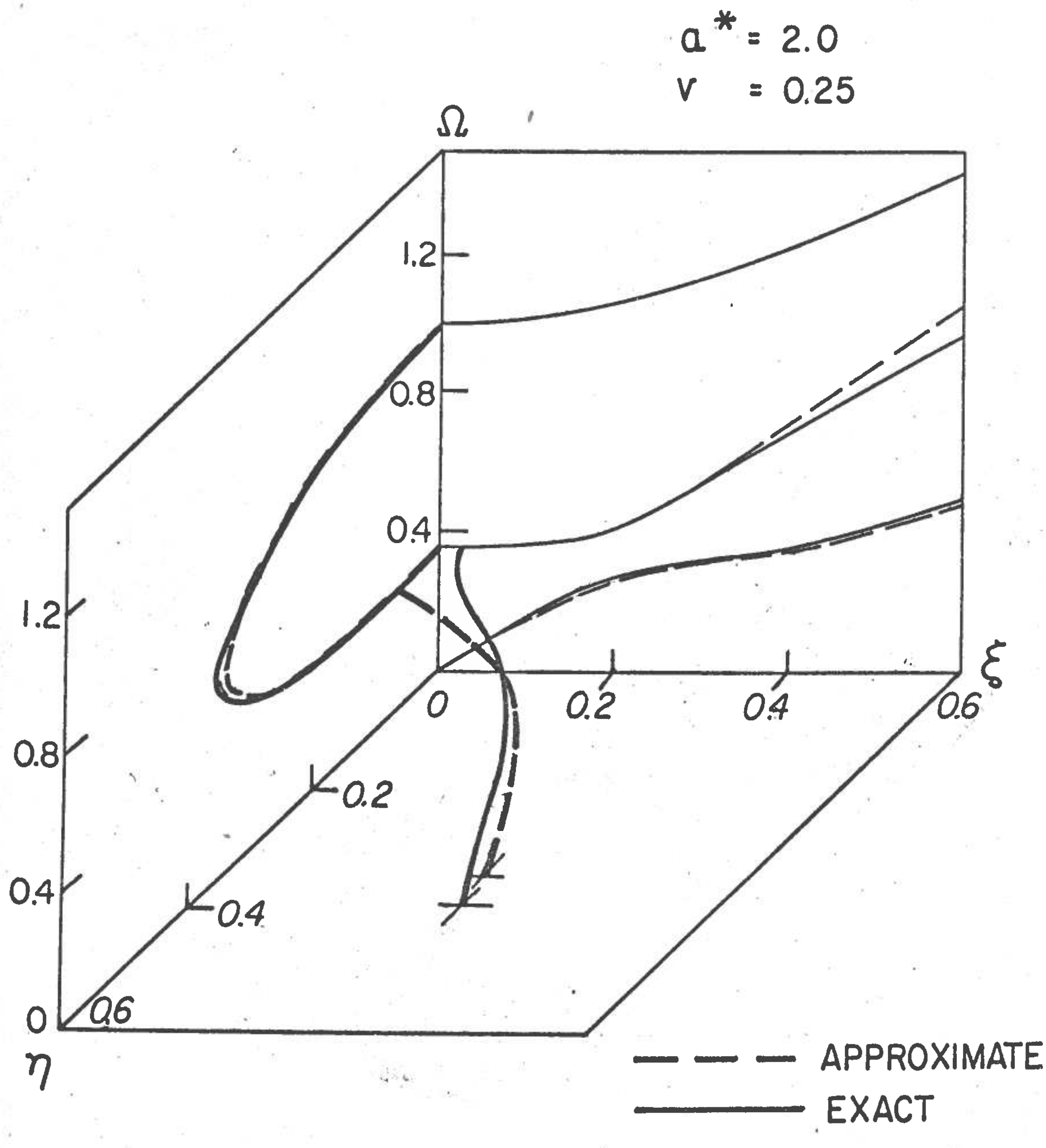
a* = 2.0
V = 0.25
Ω
1.2
0.8
0.4
1.2
0.8
0.4
0
0
0.2
0.4
0.6
ξ
0.2
0.4
0.6
η
APPROXIMATE
EXACT

FIG. 1

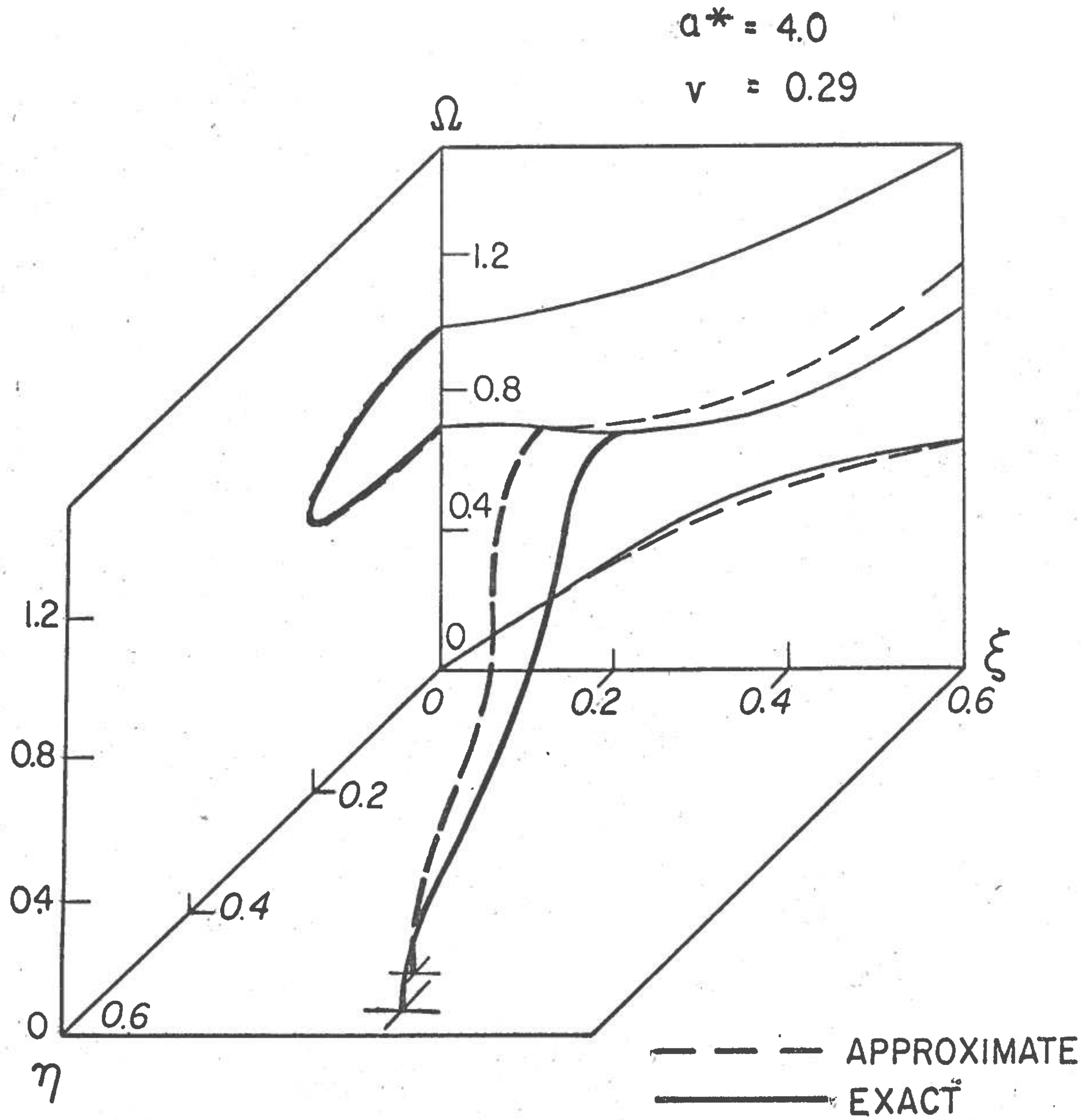
a* = 4.0
v = 0.29
Ω
1.2
0.8
0.4
0
ξ
0
0.2
0.4
0.6
1.2
0.8
0.4
0
0.2
0.4
0.6
η
APPROXIMATE
EXACT

FIG. 2

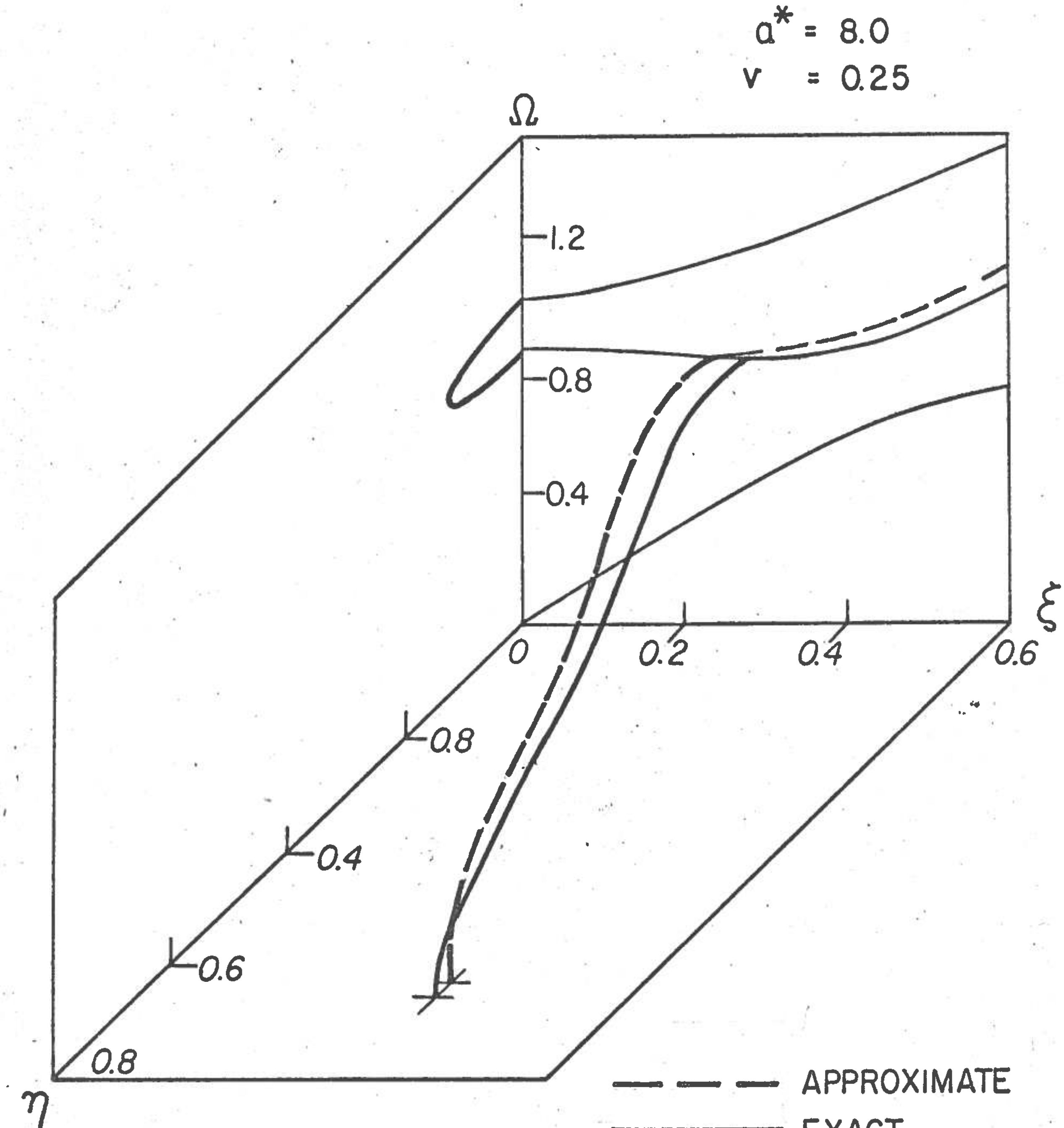

FIG. 3